Synthesis, Crystal Structure, and Magnetic Properties of a Ferrimagnetic Layered Compound $[NEt_4][Mn(5\text{-Cl-salen})]_2[Fe(CN)_6]$ (NEt_4 = Tetraethylammonium, 5-Cl-salen = *N*,*N*′-Ethylenebis((5-chlorosalicylidene)aminato))

Hitoshi Miyasaka,[†] Naohide Matsumoto,*[,†] Nazzareno Re,[‡] Emma Gallo,[§] and Carlo Floriani*[,§]

Department of Chemistry, Faculty of Science, Kyushu University, Hakozaki, Higashi-ku, Fukuoka 812, Japan, Dipartimento di Chimica, via Elce di Sotto 8, 06100 Perugia, Italy, and Institut de Chimie Minérale et Analytique, Université de Lausanne, BCH, CH-1015, Lausanne, Switzerland

Received July 24, 1996[⊗]

The discrete trinuclear complex $[(NEt_4)\{Mn(H_2O)(5\text{-Cl-salen})\}_2\{Fe(CN)_6\}]\cdot H_2O$, **3**, and a two-dimensional heterometal assembly $[(NEt_4)\{Mn(5\text{-Cl-salen})\}_2\{Fe(CN)_6\}]_n$, **4**, have been prepared (NEt_4 = tetraethylammonium, 5-Cl-salen = *N*,*N*′-ethylenebis(5-chlorosalicylidene)aminato) dianion). Compound **4** crystallizes in the monoclinic space group $P2_1/c$ with cell dimensions of $a = 13.104(3)$ Å, $b = 12.861(3)$ Å, $c = 15.526(2)$ Å, $\beta = 105.98(1)°$, $Z = 2$ and is isostructural to the previously synthesized metamagnetic compound, $[K\{Mn(3\text{-MeOsalen}\}_2\{Fe(CN)_6\}\cdot 2DMF]_n$, **5**. The structure assumes a two-dimensional network consisting of the cyclic tetramer $(-Mn-NC-Fe-CN-)_4$ as a net unit [with dimensions of Fe−C1 = 1.947(8) Å, Fe−C2 = 1.951(8) Å, Mn−N1 = 2.286(7) Å, Mn−N2 = 2.266(7) Å, Mn−N−C = 154.4(7)°, Mn−N−C = 146.1(7)°]. The magnetic study (magnetic susceptibility *vs T*, field-cooled magnetization and zero-field cooled magnetization *vs T*, hysteresis loop and saturation magnetization *vs H* up to 55 kOe) shows that the compound is a metamagnet with ferrimagnetic layers and antiferromagnetic interlayer interactions, and with a Neel temperature $T_N = 4.0$ K. The distinctly different magnetic properties of **4** and **5** are discussed and correlated with the structural parameters. The magnetic behavior of **3** was represented by the fitting parameters: $g_{Mn} = 1.98$, $g_{Fe} = 2.01$, $J = +5.9$ cm^{-1}, $D = -6.4$ cm^{-1}, $zJ' = -0.38$ cm^{-1} on the basis of a trinuclear spin system (S_{Mn} hs, S_{Fe}, S_{Mn} hs) = (2, $^1/_2$, 2) and includes a zero-field splitting term *D* and an intermolecular interaction term zJ' within the molecular field approach. The dehydration reaction of **3** in the solid state also leads to **4**.

Introduction

The molecular design of extended structures starting from molecular precursors is an area of intense interest.[1] The use of ionic building blocks, for example, in which one unit contains a potential bridging ligand and another contains a potential coordination site, can result in such molecular species. Extended bimetallic arrays assembled from hexacyanometallate and metal ions bonded to polydentate ligands, have recently received particular attention.[2] The reaction between $[Mn(BS)]^+$ [BS = salen-substituted ligand; salen = *N*,*N*′-ethylenebis(salicylideneaminato) dianion] and $[Fe(CN)_6]^{3-}$ has already led to a variety of extended structures depending on the nature of the Schiff base, which affects the steric accessibility of Mn and its coordination number.[3] The countercation and the reaction solvent can also play a significant role in the assembling process. We report here the synthesis and a structural and a magnetic study of $[(NEt_4)\{[Mn(5\text{-Cl-salen})\}_2\{Fe(CN)_6\}]_n$ [5-Cl-salen = *N*,*N*′-ethylenebis((5-chlorosalicylidene)aminato) dianion], **4**, which displays a completely different magnetic behavior from the isostructural $[K\{Mn(3\text{-MeOsalen})\}_2\{Fe(CN)_6\}\cdot 2DMF]_n$, **5**.[3] Both compounds have a two-dimensional layer-type structure made up of tetrameric cyclic units $[-Mn-C-N-Fe-C-N-]_4$, though with considerably different structural consequences. Complex **4** has a spontaneous magnetic behavior derived from an intralayer antiferromagnetic interaction between high-spin Mn(III) and low-spin Fe(III) through CN groups and an interlayer antiferromagnetic interaction. In the case of **5** there is a metamagnetic behavior as a consequence of an intralayer ferromagnetic and a weaker interlayer antiferromagnetic interaction. We also report a discrete trinuclear complex $[(NEt_4)\{[Mn(H_2O)(5\text{-Cl-salen})\}_2\{Fe(CN)_6\}]\cdot H_2O$, **3**, obtained in a different reaction solvent, and whose solid state dehydration leads again to **4**.

Experimental Section

Physical Measurements. Elemental analyses for C, H, and N were performed at the Elemental Analysis Service Centre of Kyushu University. Manganese and iron analyses were made on a Shimadzu AA-680 atomic absorption/flame emission spectrophotometer. Infrared spectra were measured on KBr disks with JASCO IR-810 and Shimadzu FTIR-8600 spectrophotometers. Thermogravimetric analysis (TGA)

[†] Kyushu University.
[‡] University of Perugia.
[§] University of Lausanne.
[⊗] Abstract published in *Advance ACS Abstracts,* January 1, 1997.

(1) (a) Kahn, O. *Molecular Magnetism*; VCH: Weinheim, Germany, 1993. (b) *Magnetic Molecular Materials*; Gatteschi, D., Kahn, O., Miller, J. S., Palacio, F., Eds.; NATO ASI Series E, Vol. 198; Kluwer: Dordrecht, The Netherlands, 1991. (c) Iwamura, H.; Miller, J. S. Proceedings of the Symposium on the Chemistry and Physics of Molecular Based Magnetic Materials; *Mol. Cryst. Liquid Cryst.* **1993**, 232−233. (d) Miller, J. S.; Epstein, A. J. *Angew. Chem., Int. Ed. Engl.* **1994**, *106*, 399. (e) Caneschi, A.; Gatteschi, D.; Sessoli, R.; Rey, P. *Acc. Chem. Res.* **1989**, *22*, 392. (f) Kahn, O. *Structure and Bonding*; Springer: Heidelberg, Germany, 1987; Vol. 68. (g) Gleizes, A.; Verdaguer, M. *J. Am. Chem. Soc.* **1981**, *103*, 7373. (h) Miller, J. S.; Epstein, A. J.; Reiff, W. M. *Chem. Rev.* **1988**, *88*, 201. (i) Chen, C.-T.; Suslick, K. S. *Coord. Chem. Rev.* **1993**, *128*, 293.

(2) (a) Ohba, M.; Maruono, N.; Okawa, H.; Enoki, T.; Latour, J. M. *J. Am. Chem. Soc.* **1994**, *116*, 11566. (b) Ohba, M.; Okawa, H.; Ito, T.; Ohto, A. *J. Chem. Soc., Chem. Commun.* **1995**, 1545.

(3) (a) Miyasaka, H.; Matsumoto, N.; Okawa, H.; Re, N.; Gallo, E.; Floriani, C. *Angew. Chem., Int. Ed. Engl.* **1995**, *34*, 1446. (b) Miyasaka, H.; Matsumoto, N.; Okawa, H.; Re, N.; Gallo, E.; Floriani, C. *J. Am. Chem. Soc.* **1996**, *118*, 981.

S0020-1669(96)00881-6 CCC: $14.00

was carried out using a Rigaku Denki TG-DTA apparatus, where the heating rate is 2.5 °C/min. Magnetic susceptibilities were measured with a Faraday balance in the temperature range 80−300 K and with a HOXSAN HSM-D SQUID magnetic susceptometer in the range 4.2−100 K; the calibrations were made with $[Ni(en)_3](S_2O_3)$ (en = ethylenediamine) for the Faraday balance and with $Mn(NH_4)_2(SO_4)_2 \cdot 6H_2O$ for the SQUID susceptometer.[4] Field cooled magnetization under 3 Oe, remnant magnetization, and zero-field cooled magnetization measurements were made on a HOXSAN HSM-D SQUID magnetic susceptometer. Field dependent magnetization measurements up to 55 kOe and at several temperatures were made on a MPMS5 SQUID susceptometer (Quantum Design Inc.). Corrections were applied for diamagnetism calculated from Pascal's constants.[5] Effective magnetic moments were calculated by the equation $\mu_{eff} = 2.828\ (\chi_M \times T)^{1/2}$, where χ_M is the magnetic susceptibility per formula unit.

X-ray Data Collection, Reduction, and Structure Determination. Single crystals of **4** were prepared by the diffusion method described in the synthetic procedure. The single crystal was cut from a thin plate crystal, mounted on a glass rod, and coated with epoxy. Crystal dimensions are 0.35 × 0.08 × 0.25 mm. All measurements were made on a Rigaku AFC7R diffractometer with graphite monochromated Mo Kα radiation ($\lambda = 0.710\ 69$ Å) and a 12 kW rotating anode generator. The data were collected at a temperature of 20 ± 1 °C (using the $\omega-2\theta$ scan technique) to a maximum 2θ value of 50.0° at a scan speed of 16.0°/min (in ω). The weak reflections ($I < 10.0\sigma(I)$) were rescanned (maximum of four scans), and the counts were accumulated to ensure good counting statistics. Stationary background counts were recorded on each side of the reflection. The ratio of peak counting time to background counting time was 2:1. Of the 5059 reflections which were collected, 4656 were unique. The diameter of the incident beam collimator was 1.0 mm, the crystal to detector distance was 235 mm, and the computer-controlled detector aperture was set to 9.0 × 13.0 mm (horizontal × vertical). The intensities of three representative reflections were measured after every 150 reflections. Over the course of the data collection, the standards reflections were monitored and the decay corrections were applied by a polynomial correction. An empirical absorption correction based on azimuthal scans of several reflections was applied. The data were corrected for Lorentz and polarization effects.

The structure was solved by direct methods[6] and expanded using Fourier techniques.[7] The non-hydrogen atoms were refined anisotropically. Hydrogen atoms were placed in idealized positions. Final refinement was done by full-matrix least-squares procedures using anisotropic thermal parameters for non-hydrogen atoms and isotropic ones for hydrogen atoms. Full-matrix least-squares refinement based on 2482 observed reflections ($I > 3.00\sigma(I)$) was employed, where the unweighted and weighted agreement factors of $R = \sum||F_o| - |F_c||/\sum|F_o|$ and $R_w = [\sum w(|F_o| - |F_c|)^2/\sum w|F_o|^2]^{1/2}$ are used. The weighting scheme was based on counting statistics. Plots of $\sum w(|F_o| - |F_c|)^2$ *vs* $|F_o|$, reflection order in data collection, sin θ/λ, and various classes of indices showed no unusual trends. Neutral atomic scattering factors were taken from Cromer and Waber.[8] Anomalous dispersion effects were included in F_{calcd}; the values $\Delta f'$ and $\Delta f''$ were those of Creagh and McAuley.[9a] The values for the mass attenuation coefficients are those of Creagh and Hubbel.[9b] All calculations were performed using the teXsan crystallographic software package of the Molecular Structure Corporation.[10]

Table 1. Crystallographic Data for **4** and **5**[2]

compd	4	5
Formula	$C_{46}H_{44}N_{11}Cl_4FeMn_2O_4$	$C_{48}H_{50}KFeMn_2N_{12}O_{10}$
fw	1122.46	1159.82
Cryst Syst	monoclinic	monoclinic
space group	$P2_1/c$	$P2_1/c$
T, °C	20	20
λ, Å	0.710 69	0.710 69
a, Å	13.104(3)	13.750(4)
b, Å	12.861(3)	12.456(2)
c, Å	15.526(2)	15.646(2)
α, deg	90	90
β, deg	105.98(1)	102.91(1)
γ, deg	90	90
V, Å^3	2515.3(8)	2612.1(9)
Z	2	2
D_{calcd}, g cm^{-3}	1.482	1.475
D_m, g cm^{-3}	1.48	1.49
μ(Mo Kα), cm^{-1}	10.44	8.97
R[a]	5.3	4.9
R_w[a]	5.2	5.0

[a] $R = \sum||F_o| - |F_c||/\sum|F_o|$, $R_w = \{\sum[w(|F_o| - |F_c|)^2]/\sum[w|F_o|^2]\}^{1/2}$, $w = 1/\sigma(F_o)^2$. The densities were measured by the floatation method in a mixed solution of benzene and tetrachloromethane.

Crystal data and details of the structure determination of the complex **4**, together with those of a metamagnet **5**, are summarized in Table 1.

Warning! Perchlorate salts are potentially explosive and should only be handled in small quantities.

General Procedures and Materials. All chemicals and solvents used for the synthesis were reagent grade. The quadridentate Schiff base ligand 5-Cl-salenH_2 was prepared by mixing 5-chlorosalicylaldehyde and ethylenediamine with the mole ratio of 2:1 in methanol, as described elsewhere.[11] $[Mn(5\text{-Cl-salen})(H_2O)]ClO_4$, **1**, was prepared by mixing $Mn(OAc)_3 \cdot 2H_2O$, 5-Cl-salenH_2, and $NaClO_4$ with the molar ratio of 1:1:1.5 in methanol/H_2O according to the literature method.[12] $[NEt_4]_3[Fe(CN)_6]$, **2**, was prepared according to the literature.[13] Since $[NEt_4]_3[Fe(CN)_6]$ has a tendency to decompose on heating and irradiation, the synthesis was performed at room temperature and crystallization was performed in the dark.

The assembly reaction of $[Mn(5\text{-Cl-salen})(H_2O)]ClO_4$, **1**, and $[NEt_4]_3[Fe(CN)_6]$, **2**, was carried out either by mixing the methanolic solutions of the two component compounds or by the diffusion method. The two methods gave slightly different products with respect to the content of water of crystallization.

Preparation of 3. To a solution of **1** (0.25 g, 0.5 mmol) in methanol (30 mL) was added a solution of **2** (0.30 g, 0.5 mmol) in methanol (20 mL) at room temperature. The resulting solution was filtered, and the filtrate was kept overnight in an ice bath kept in the dark. The resulting yellowish brown precipitate was then collected by filtration, washed with methanol, and dried *in vacuo*. Anal. Calcd for $C_{46}H_{50}Cl_4FeMn_2N_{11}O_7$: C, 46.96; H, 4.28; N, 13.10; Mn, 9.34. Found: C, 46.99; H, 4.16; N, 12.94; Mn, 8.97. IR (KBr): νC═N (imine), 1600 (sh), 1632 cm^{-1}; νC≡N (cyanide), 2108 cm^{-1}. Mp: >300 °C.

Preparation of 4. Into a solution of **1** (0.25 g, 0.5 mmol) in DMF (30 mL) was diffused a solution of **2** (0.30 g, 0.5 mmol) in 30 mL of 2-propanol and acetonitrile. After the solution stood for 1 week at

(4) Lindoy, L. F.; Katovic, V.; Busch, D. H. *J. Chem. Educ.* **1972**, *49*, 117.
(5) Boudreaux, E. A.; Mulay, L. N. In *Theory and Applications of Molecular Paramagnetism*, Wiley: New York, 1976; pp 491−495.
(6) SAPI91: Fan Hai-Fu, Structure Analysis Programs with Intelligent Control, Rigaku Corporation, Tokyo, Japan, 1991. MULTAN88: Debaerdemaeker, T.; Germain, G.; Main, P.; Refaat, L. S.; Tate, C.; Woolfson, M. M. Computer program for the automatic solution of crystal structures from X-ray diffraction data, University of York: York, U.K., 1988. SHELXS86: Sheldrick, G. M. A program for X-ray crystal structure determination, University of Cambridge: Cambridge, U.K., 1986.
(7) DIRDIF92: Beurskens, P. T.; Admiraal, G.; Beurskens, G.; Bosman, W. P.; Garcia-Granda, S.; Gould, R. O.; Smits, J. M. M.; Smykalla, C. The DIRDIF program system, Technical Report of the Crystallography Laboratory, University of Nijmegen: The Netherlands, 1992.
(8) Cromer, D. T.; Waber, J. T. *International Tables for X-ray Crystallography*; The Kynoch Press: Birmingham, U.K., 1974; Vol. IV, Table 2.2A.
(9) (a) Creagh, D. C.; McAuley, W. J. In *International Tables for Crystallography*; Wilson, A. J. C., Ed., Kluwer: Boston, 1992; Vol. C, Table 4.2.6.8, pp 219−222. (b) Creagh, D. C.; Hubbel, J. H. In *International Tables for Crystallography*; Wilson, A. J. C., Ed.; Kluwer: Boston, 1992; Vol. C, Table 4.2.4.3, pp 200−206.
(10) teXsan: Crystal Structure Analysis Package, Molecular Structure Corporation, 1985, 1992.
(11) (a) McCarthy, P. J.; Hovey, R. J.; Ueno, K.; Martell, A. E. *J. Am. Chem. Soc.* **1955**, *77*, 5820. (b) Pfeifer, P.; Hesse, T.; Pfitzner, H.; Scholl, W.; Thielert, H. *J. Prakt. Chem.* **1937**, *149*, 217.
(12) Matsumoto, N.; Takemoto, N.; Ohyoshi, A.; Ōkawa, H. *Bull. Chem. Soc. Jpn.* **1988**, *61*, 2984.
(13) Mascharak, P. K. *Inorg. Chem.* **1986**, *25*, 245.

Scheme 1

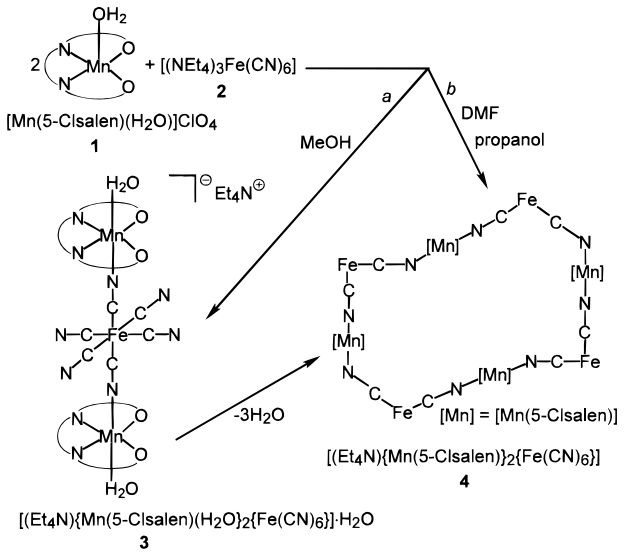

room temperature and in the dark, the formation of dark brown plate crystals, which were collected by filtration, washed with 2-propanol, and dried in air, resulted. Anal. Calcd for $C_{46}H_{44}Cl_4FeMn_2N_{11}O_4$: C, 46.22; H, 3.95; Fe, 4.98; Mn, 9.79; N, 13.73. Found: C, 46.16; H, 3.94; Fe, 4.61; Mn, 9.77; N, 13.70. IR (KBr): νC═N (imine), 1599, 1645 cm^{-1}; νC≡N (cyanide), 2116 cm^{-1}. Mp: >300 °C.

Dehydration of 3. Compound **3** has the formula of $[(NEt_4)\{Mn(H_2O)(5\text{-Cl-salen})\}_2\{Fe(CN)_6\}]\cdot H_2O$. In a procedure monitored by thermogravimetric analysis, with a testing rate of 2.5 °C/min, one of the three water molecules is lost at 35−50 °C, and the two remaining molecules at 85−115 °C. The compound decomposed at 218 °C. The dehydrated compound was prepared by heating **3** (0.145 g) at 150 °C. The resulting sample was characterized by IR and magnetic measurements. Both the IR spectrum and the μ_{eff} *vs T* plots are superimposable with those for **4**, clearly indicating that the solid state dehydration of **3** leads to **4**. IR (KBr): νC═N (imine), 1600, 1632 cm^{-1}; νC≡N (cyanide), 2116 cm^{-1}.

Results

Synthesis and Characterization of 3 and 4. The synthesis of oligomeric/polymeric chain-like aggregates containing the [Mn−N−C−Fe] linkage has been carried out according to the strategies shown in Scheme 1. Reactions (pathway *a*) carried out by mixing methanolic solutions of **1**, $[Mn(5\text{-Cl-salen})(H_2O)](ClO_4)$ with **2**, resulted in the trinuclear hydrated complex **3**. This hydrated complex underwent a complete thermal dehydration to **4**, as evidenced by IR and magnetic measurements. One of the three molecules of H_2O corresponding to the water of crystallization is lost at 35−50 °C while the remaining two, which correspond to water molecules coordinated to the Mn ions, are lost at 85−115 °C. The dehydration of **3** from a coordination site on each Mn led to the polymerization of the trinuclear unit into a two-dimensional network, which has the repeating cyclic unit shown in Scheme 1 for **4**.[14] The same dehydrated form **4** has been obtained by allowing a solution of **1** in DMF to diffuse into a solution of **2** in 2-propanol and acetonitrile. Compound **4** has been obtained as brown thin plates, which do not retain any solvent of crystallization. These crystals were used in the X-ray analysis.

Structural Analysis of 4. An ORTEP view of the trimetallic anion and the tetraethylammonium cation with the numbering scheme of the unique atoms is shown in Figure 1. The central

(14) The details on the formation of extended structures from discrete oligomeric species in the solid states will be reported in a forthcoming paper.

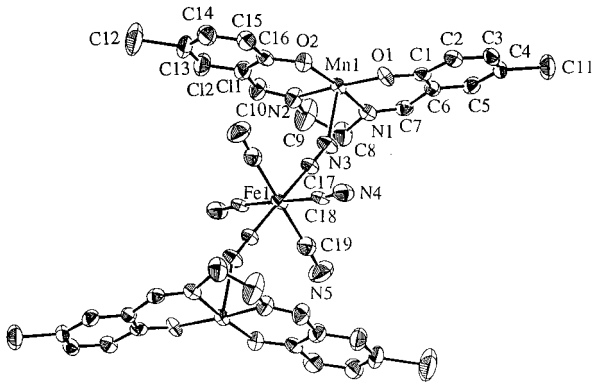

Figure 1. An ORTEP drawing of a trinuclear structure $[Mn(5\text{-Clsalen})]_2[Fe(CN)_6]^-$ and NEt_4^+ cation with the atom numbering scheme of the unique atoms, showing 50% probability ellipsoids.

Table 2. Fractional Positional Parameters and Equivalent Isotropic Thermal Parameters for Non-Hydrogen Atoms for **4**

atom	*x*	*y*	*z*	*B*(eq)
Fe	1/2	0	1/2	2.34(4)
Mn(1)	0.5014(1)	−0.1899(1)	0.203 39(8)	2.26(3)
Cl(1)	0.9049(2)	−0.0988(2)	−0.0251(2)	5.27(7)
Cl(2)	−0.0030(2)	−0.3097(3)	0.2876(2)	8.6(1)
O(1)	0.5515(4)	−0.0841(4)	0.1395(3)	2.7(1)
O(2)	0.3608(4)	−0.1387(4)	0.1834(4)	2.9(1)
N(1)	0.6433(5)	−0.2584(5)	0.2336(4)	2.7(2)
N(2)	0.4716(5)	−0.3130(5)	0.2687(5)	3.3(2)
N(3)	0.5485(6)	−0.1050(5)	0.3379(4)	3.4(2)
N(4)	0.5442(6)	0.2116(5)	0.4224(4)	3.8(2)
N(5)	0.7325(6)	−0.0343(7)	0.6120(6)	5.5(2)
N(6)	0	0	1/2	6.1(4)
C(1)	0.6316(6)	−0.0892(6)	0.1034(5)	2.5(2)
C(2)	0.6431(6)	−0.0131(6)	0.0421(5)	2.8(2)
C(3)	0.7257(7)	−0.0139(7)	0.0036(5)	3.1(2)
C(4)	0.8006(6)	−0.0930(7)	0.0245(5)	3.0(2)
C(5)	0.7940(6)	−0.1687(6)	0.0839(5)	3.0(2)
C(6)	0.7106(6)	−0.1667(6)	0.1251(5)	2.5(2)
C(7)	0.7135(6)	−0.2447(7)	0.1914(5)	2.7(2)
C(8)	0.6559(8)	−0.3373(8)	0.3034(7)	5.0(3)
C(9)	0.5596(8)	−0.3885(8)	0.2954(8)	6.5(3)
C(10)	0.3833(7)	−0.3367(7)	0.2834(6)	3.9(2)
C(11)	0.2889(7)	−0.2737(7)	0.2569(6)	3.6(2)
C(12)	0.2006(8)	−0.3136(8)	0.2809(6)	4.7(3)
C(13)	0.1063(8)	−0.2590(9)	0.2581(7)	5.0(3)
C(14)	0.0992(7)	−0.1649(8)	0.2127(6)	4.3(3)
C(15)	0.1855(7)	−0.1260(7)	0.1889(6)	3.7(2)
C(16)	0.2815(7)	−0.1793(6)	0.2091(5)	2.6(2)
C(17)	0.5324(6)	−0.0673(6)	0.3984(5)	2.5(2)
C(18)	0.5320(7)	0.1343(6)	0.4550(5)	2.6(2)
C(19)	0.6492(7)	−0.0197(7)	0.5712(6)	3.4(2)

[a] $B(\text{eq}) = (8\pi^2/3)(U_{11}(aa^*)^2 + U_{22}(bb^*)^2 + U_{33}(cc^*)^2 + 2U_{12}aa^*bb^* \cos\gamma + 2U_{13}aa^*cc^* \cos\beta + 2U_{23}bb^*cc^* \cos\alpha)$.

Fe ion and the nitrogen atom of $[NEt_4]^+$ are positioned at the inversion centers with the carbon atoms of $[NEt_4]^+$ suffering from disorder. The bond distances and angles are reported in Table 2. Figure 2 shows a view projected along the *a*-axis of the two-dimensional network layered structure and consists of a cyclic tetramer $[-Mn-NC-Fe-CN-]_4$ as the net unit.

Complex **4** is isostructural to **5** and has a metamagnetic behavior. The fact that the two isostructural compounds display very different magnetic behavior prompted us to compare the structural parameters of the two compounds in order to arrive at a structure−property relationship. In this comparison, the same numbering scheme is used for both compounds; the relevant bond distances and angles of the network structure for **4** and **5** are listed in Table 3. In complex **4**, iron occupies the inversion centers, (1/2,0,1/2), and two CN^- groups of the $[Fe(CN)_6]^{3-}$ moiety bridge the Mn ions resulting in a linear

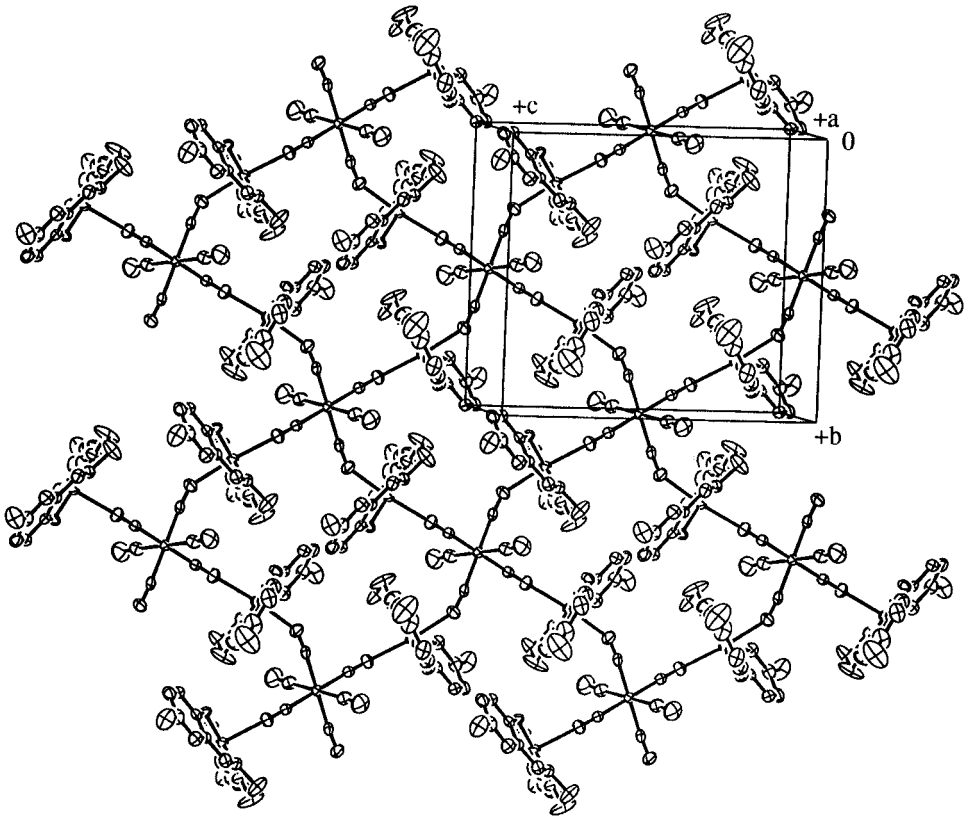

Figure 2. Two-dimensional network structure of **4** comprising of a cyclic octanuclear structure (−Mn−NC−Fe−CN−)4 as a net unit.

Table 3. Relevant Bond Distances (Å) and Angles (deg) for **4** with the Estimated Standard Deviations in Parentheses

Fe−C(17)	1.947(8)	N(4)−C(18)	1.146(9)
Fe−C(18)	1.951(8)	N(5)−C(19)	1.12(1)
Fe−C(19)	1.979(9)	C(1)−C(2)	1.40(1)
Mn−O(1)	1.904(5)	C(1)−C(6)	1.41(1)
Mn−O(2)	1.901(5)	C(2)−C(3)	1.37(1)
Mn−N(1)	1.993(7)	C(3)−C(4)	1.39(1)
Mn−N(2)	1.976(7)	C(4)−C(5)	1.36(1)
Mn−N(3)	2.286(7)	C(5)−C(6)	1.41(1)
Mn−N(4)	2.266(7)	C(6)−C(7)	1.43(1)
Cl(1)−C(4)	1.746(8)	C(8)−C(9)	1.40(1)
Cl(2)−C(13)	1.747(9)	C(10)−C(11)	1.44(1)
O(1)−C(1)	1.320(9)	C(11)−C(12)	1.41(1)
O(2)−C(16)	1.318(9)	C(11)−C(16)	1.41(1)
N(1)−C(7)	1.279(9)	C(12)−C(13)	1.38(1)
N(1)−C(8)	1.46(1)	C(13)−C(14)	1.39(1)
N(2)−C(9)	1.48(1)	C(14)−C(15)	1.38(1)
N(2)−C(10)	1.28(1)	C(15)−C(16)	1.39(1)
N(3)−C(17)	1.126(9)		
Mn(1)−N(3)−C(17)	154.4(7)	Mn(1)−N(4)−C(18)	146.1(7)
Fe(1)−C(17)−N(3)	177.9(8)	Fe(1)−C(18)−N(4)	174.4(8)

Table 4. Comparison of Relevant Bond Distances and Angles of the Cyclic Tetrameric Unit [−Mn−N(1)−C(1)−Fe−C(2)−N(2)−]4 for **4** and **5** (Estimated Standard Deviations in Parentheses)

compd	**4**	**5**
Fe−C(1)	1.947(8)	1.932(5)
Fe−C(2)	1.951(8)	1.943(6)
Mn−N(1)	2.286(7)	2.290(5)
Mn−N(2)	2.266(7)	2.415(5)
Mn−N(1)−C(1)	154.4(7)	169.5(5)
Mn−N(2)−C(2)	146.1(7)	137.2(4)

trinuclear unit, Mn−NC−Fe−CN−Mn [Fe−C(17), 1.947(8); Mn−N(3), 2.286(7); C(17)−N(3), 1.126(9) Å; Fe−C(17)−N(3), 177.9(8)°; C(17)−N(3)−Mn, 154.4(7)°]. Two other CN^- groups from $[Fe(CN)_6]^{3-}$ are bonded to the Mn ions of the adjacent trinuclear units [Mn*−N(4), 2.266(7); N(4)−C(18), 1.146(9) Å; Mn*−N(4)−C(18), 146.1(7)°, Fe−C(18)−N(4), 174.4(8)°]. This Fe−C−N−Mn interaction produces a two-dimensional network with a repeating cyclic tetrameric [Mn−NC−Fe−CN]4 unit. Due to coordination of the CN^- groups, the Mn ion assumes an octahedral geometry, with the two apical sites occupied by N(3) and N(4)* [the asterisk (*) denotes the atom of an adjacent unit; Mn−N(3), 2.286(7), Mn−N(4)*, 2.266(7) Å] and the equatorial plane by the N_2O_2 set of donor atoms from the salen ligand. The intertrimer Mn−N distances in **4** and **5** are very different, with the distance in **5** much longer than that in **4** [Mn−N(3), 2.290(5) Å for **4**, Mn−N(4)*, 2.415(5) Å for **5**]. The intratrimer distances are quite similar. In addition, the two structures show different C−N−Mn angles within the octanuclear unit [C(17)−N(3)−Mn, 154.4(7)° and Mn*−N(4)−C(18), 146.1(7)° in **4** *vs* 169.5(5)° and 137.2(4)° in **5**].

As shown in Figure 2, the two-dimensional layer structure stacks along the *a*-axis by a transformation and the $[NEt_4]^+$ cation is positioned at the inversion center between the layers, while in **5** the K^+ ion occupies the center of the octanuclear ring of a layer. In the latter case, K^+ interacts with eight oxygen atoms from two [Mn(3-MeOsalen)] moieties of adjacent trinuclear units. As is true for the noninteracting $[NEt_4]^+$ (mentioned above), the cyclic octanuclear unit shows a regular trend in the structural parameters, whereas in **5** it is probable that the K^+ cation, interacting with the two [Mn(3-MeOsalen)] moieties, causes significant distortions in the intertrimer Mn−N and C−N−Mn parameters.

Magnetic Properties of 3. The magnetic susceptibility was measured from 4.4 to 300 K, and the resulting plots of μ_{eff} *vs* *T* and $1/\chi_M$ *vs* *T* are given in Figure 3. The plots of $1/\chi_M$ *vs* *T* above 30 K obey the Curie−Weiss law with a positive Weiss constant of $\Theta = +1.4$ K, indicating the presence of a ferromagnetic interaction. The μ_{eff} at room temperature, 7.18 μ_B, is compatible with the spin-only value of 7.14 μ_B expected

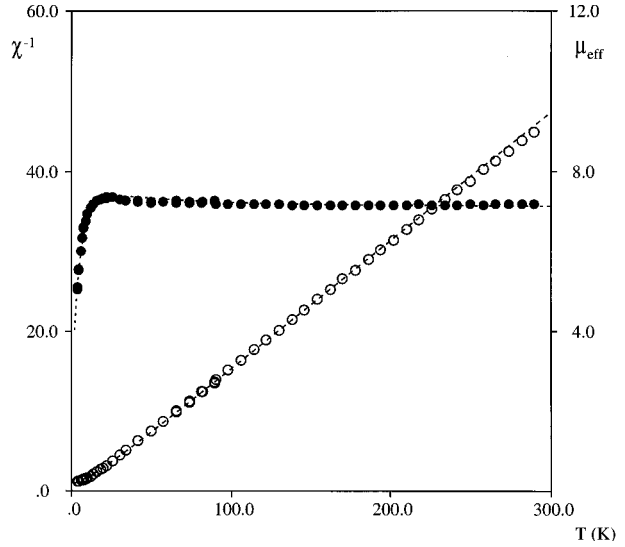

Figure 3. Plots of μ_{eff} *vs T* and $1/\chi_M$ *vs T* for **3**, where the measurement was carried out under the applied magnetic field of 100 Oe, and μ_{eff} and χ_M denote the effective magnetic moment and magnetic susceptibility per trinuclear unit, respectively. The dotted line of the μ_{eff} *vs T* plot represents a theoretical curve with the fitting parameters of $g_{Mn} = 2.01$, $g_{Fe} = 1.98$, $J = +5.9$ cm^{-1}, $D = -6.4$ cm^{-1}, $zJ' = -0.38$ cm^{-1}.

for the magnetically dilute spin system (S_{Mn} hs, S_{Fe}, S_{Mn} hs) = (2, $^1/_2$, 2), where the spin-only value was calculated by assuming $g_{Mn} = 2.00$ and $g_{Fe} = 2.00$. Lowering the temperature results in a gradual increase in μ_{eff} to give a maximum of 7.37 μ_B at 26 K, followed by a decrease. This behavior suggests that the compound is a discrete trinuclear Mn(III)−Fe(III)−Mn(III) species with ferromagnetic Mn(III)−Fe(III) coupling. The decrease at low temperature is due to the zero-field splitting of the manganese(III) ion. The magnetic behavior is well reproduced by the following spin Hamiltonian

$$H = \beta H(2g_{Mn}S_{Mn} + g_{Fe}S_{Fe}) - 2J(S_{Mn1}S_{Fe} + S_{Mn2}S_{Fe}) + D[S_z^2 - S_{Mn}(S_{Mn} + 1)/3] - zJ'\langle S\rangle$$

based on a symmetric linear trinuclear structure with the spin system (S_{Mn} hs, S_{Fe}, S_{Mn} hs) = (2, $^1/_2$, 2) and includes a zero-field splitting term and an intermolecular interaction term within the molecular field approach. The best-fit parameters are $g_{Mn} = 2.01$, $g_{Fe} = 1.98$, $J = +5.9$ cm^{-1}, $D = -6.4$ cm^{-1}, $zJ' = -0.4$ cm^{-1} and lead to the theoretical curve represented as a solid line in Figure 3. The above parameters are compatible with those of the potassium salt $[K\{Mn(5\text{-Cl-salen})(H_2O)\}_2\{Fe(CN)_6\}]_n$ reported previously ($J = +4.2$ cm^{-1}, $zJ' = -0.3$ cm^{-1}, $g_{Mn} = 2.04$, $g_{Fe} = 2.04$, $D = -7.8$ cm^{-1}), indicating an intramolecular ferromagnetic coupling between Mn(III) and Fe(III) ions and a large zero-field splitting. The magnetic results indicate that the compound is a discrete trinuclear Mn(III)−Fe(III)−Mn(III) complex.

Magnetic Properties of 4. The plots of μ_{eff} *vs T* and $1/\chi_M$ *vs T* are given in Figure 4. The plot of $1/\chi_M$ *vs T* above 30 K obeys the Curie−Weiss law with a negative Weiss constant of $\Theta = -19.2$ K, indicating the presence of an antiferromagnetic interaction. The μ_{eff} at room temperature, 7.42 μ_B, is slightly larger than the spin-only value of 7.14 μ_B expected for the magnetically dilute spin system (S_{Mn} hs, S_{Fe}, S_{Mn} hs) = (2, $^1/_2$, 2) assuming $g_{Mn} = 2.00$ and $g_{Fe} = 2.00$, probably because of an orbital contribution to the magnetic moment of the low-spin Fe(III) ion. On lowering the temperature, μ_{eff} gradually decreases and shows a minimum of 6.10 μ_B at ca 30 K, then increases abruptly to reach a maximum of 40.8 μ_B at 10.1 K

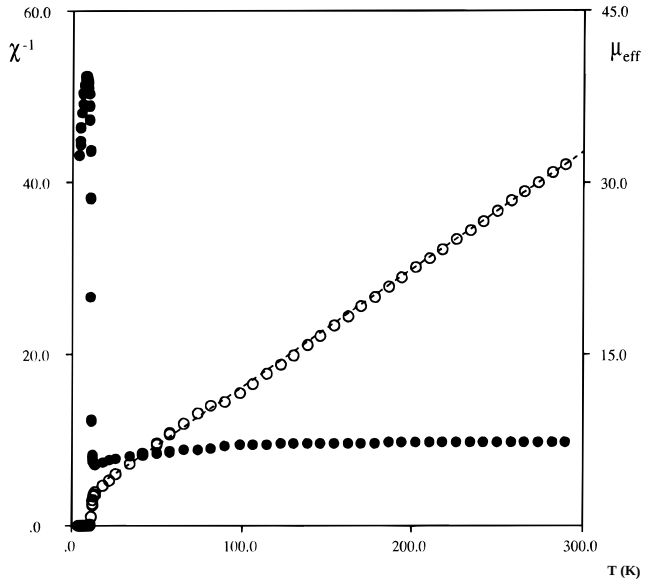

Figure 4. Plots of μ_{eff} *vs T* and $1/\chi_M$ *vs T* for **4**, where the measurement was carried out under the applied magnetic field of 100 Oe, and μ_{eff} and χ_M denote the effective magnetic moment and magnetic susceptibility per trinuclear unit, respectively.

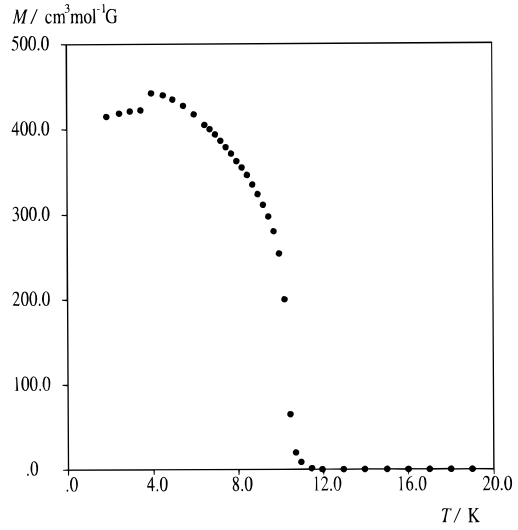

Figure 5. FCM (field cooled magnetization *vs T*) curve under a weak magnetic field 3 Oe for **4**.

and finally decreases sharply to 32.9 μ_B at 4.4 K. The presence of a minimum followed by a sudden increase suggests that an antiferromagnetic interaction operates between the high-spin Mn(III) ions of the [Mn(5-Cl-salen)] components and the low-spin Fe(III) ions of the $[Fe(CN)_6]^{3-}$ components *via* a bridging CN^- group. As a consequence, an intralayer ferrimagnetic ordering is obtained.

The abrupt increase of μ_{eff} below 30 K suggests the onset of magnetic ordering. To confirm the magnetic phase transition, the FCM (field cooled magnetization) curve *vs T* was measured under a weak magnetic field of 3 Oe and is given in Figure 5. On lowering the temperature, the FCM curve under 3 Oe shows a rapid increase below *ca.* 11 K with a saturation of 450 cm^3 mol^{-1} Oe around 5 K. It then shows a slight decrease below 4.0 K. The abrupt increase of the magnetization below 11 K in the FCM curve indicates the onset of long-range magnetic ordering due to the ferrimagnetic coupling within each layer while the small decrease below 4.0 K suggests the presence of a weak antiferromagnetic interlayer interaction. This latter effect is better seen by studying the zero-field cooled magnetization (ZFCM) as a function of the temperature. Two ZFCM curves

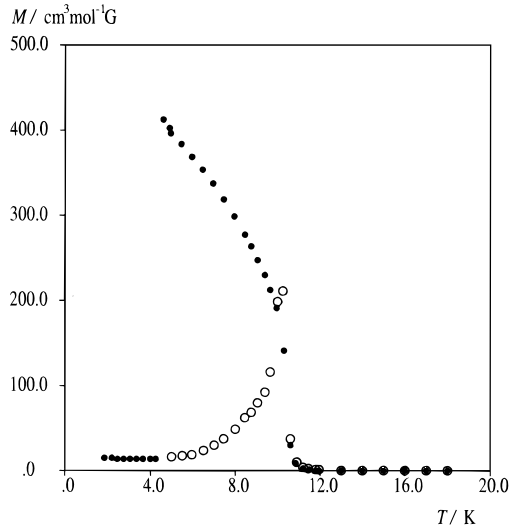

Figure 6. ZFCM (zero-field cooled magnetization) for **4**, cooled down to (a) 5 K, ○, and (b) 1.9 K, ●.

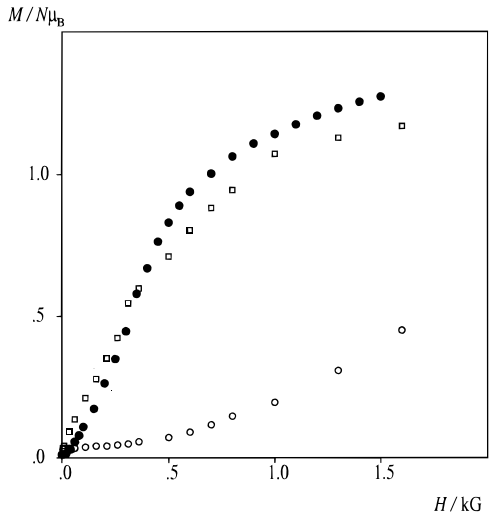

Figure 7. Magnetization as a function of the applied magnetic field up to 1.6 kOe for **4**, performed at 1.9 K, ○; 4.5 K, ●; and 8 K, □.

were obtained by cooling the sample under zero field to two different temperatures and measuring the magnetization on heating. If the sample is cooled to 5 K, then the ZFCM curve steadly increases until a peak is reached at 10.3 K and then disappears on further warming (Figure 6a). If the sample is cooled to 1.9 K, the ZFCM curve has a plateau in the range 1.9−4.3 K followed by a sudden discontinuous increase at 4.6 K and then a stead decrease on warming, which disappears above 11 K (Figure 6b). The former ZFCM curve shows the typical behavior expected for a polycrystalline ferrimagnet, while the latter curve clearly indicates that below 4.3 K the layers are antiferromagnetically coupled and confirms the metamagnetic character of **4**. This behavior was better characterized by investigating the magnetization as a function of the external magnetic field at various temperatures, above and below the Neel temperature, *ca.* 4 K. The results are reported in Figure 7 and show that only curves below 4 K have the sigmoidal shape expected for a metamagnet, with a critical field around 2 kOe obtained at the lowest temperature of 1.9 K. Curves between 4 and 11 K do not have a sigmoidal shape, but show a gradual increase with a slope much smaller than that expected for a true ferrimagnet. Hysteresis loops have been observed above 4 K, and that measured at 5 K is reported in Figure 8.

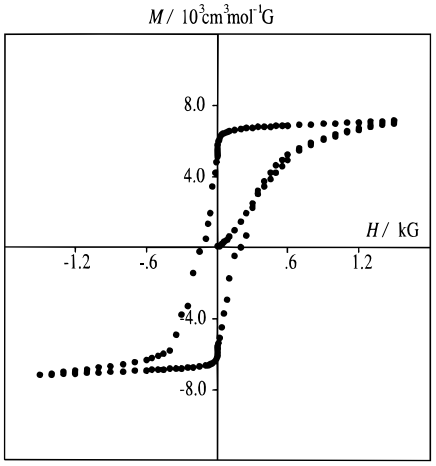

Figure 8. Hysteresis loop at 5.0 K of **4**.

The field dependence of the magnetization up to 55 kOe was measured at 1.9, 4.5, and 6 K. The curve at 1.9 K is sigmoidal at low fields (see Figure 7), but the slope increases dramatically above 2 kOe. When the field is further increased, the magnetization shows a slower, almost linear, increase and is still rising at the highest measured field (55 kOe), indicating that the expected saturation value of 7 N μ_B ($= 2g_{Mn}S_{Mn} - g_{Fe}S_{Fe}$) has not yet been reached. The magnetization curves taken at 4.5 and 6 K, show a rapid increase at low fields, with an extremely large zero-field susceptibility, to reach a plateau of about 1.7 N μ_B. However, the behavior at a higher field is similar to that observed at 1.9 K, with a gradual increase of the magnetization up to about 4 N μ_B at 55 kOe. This gradual increase is typical of systems with a significant anisotropy due to a large zero-field splitting and is consistent with the high values (up to several cm^{-1}) observed for Mn(III) ions in analogous Schiff bases compounds.[15] It is also worth noting that the magnetization rises more rapidly as the temperature increases, which is typical of a metamagnetic character.

Discussion

Examination of the structural parameters of the isostructural compounds **4** and **5** has led us to propose a structure−property correlation for the different magnetic behavior. Both compounds crystallize in the same space group $P2_1/c$ with quite similar cell dimensions. Both structures are made up by the same repeating unit, that is the tetrameric [Mn−NC−Fe−CN]$_4$ ring. Although the overall structure is the same for both compounds, the structural parameters of the repeating octanuclear unit are affected by the K^+ countercation bonded to the oxygens of the Schiff base in **5** which causes the major distortions [Mn−N(1), 2.290(5) Å, Mn−N(2), 2.415(5) Å, Mn−N−C, 169.5(5)°, M−N−C, 137.2(4)° for **5**; Mn−N(1), 2.286(7) Å, Mn−N(2), 2.266(7) Å, Mn−N−C = 154.4(7)°, M−N−C, 146.1(7)° for **4**] (see the previous section).

This makes a significant difference in the structural interpretation and in the magnetic behavior of these complexes. In **5** the structural network can be considered as CN^- bridged Mn(III)−Fe(III)−Mn(III) trinuclear units which slightly interact through two different CN^- ligands of the central $[Fe(CN)_6]^{3-}$ building block,[2] while in **4** all the CN^- bridged Mn(III)−Fe(III)

(15) (a) Boucher, L. J.; Coe, C. G. *Inorg. Chem.* **1975**, *14*, 1289. (b) Bertoncello, K.; Fallon, G. D.; Murray, K. S.; Tiekink, R. T. *Inorg. Chem.* **1991**, *30*, 3562. (c) Chandra, S. K.; Chakraborty, P.; Chakravorty, A. *J. Chem. Soc., Dalton Trans.* **1993**, 863. (d) Bonadies, J. A.; Kirk, M. L.; Lah, M. S.; Kessissoglou, D. P., Hatfield, W. E.; Pecoraro, V. L. *Inorg. Chem.* **1989**, *28*, 2037. (e) Kennedy, B. J.; Murray, K. S. *Inorg. Chem.* **1985**, *24*, 1552.

interactions are essentially equivalent so that each Fe(III) ion at the corners of the $(-Mn-NC-Fe-CN-)_4$ tetramer interacts equivalently with four Mn(III) ions.

Further, the magnetic data indicate that both intratrimer and intertrimer magnetic interactions between Mn(III) and Fe(III) and *via* a CN^- group are ferromagnetic for **5**, while all the Mn(III)−Fe(III) interactions of **4** are antiferromagnetic.

The deformation of the octanuclear unit therefore has a profound effect on the exchange coupling between Fe(III) and Mn(III), which is antiferromagnetic in **4** and ferromagnetic in **5**. It would be interesting to consider possible orbital explanations for the differences in the intralayer magnetic coupling of **4** and **5**. In a simple orbital scheme of exchange between two magnetic centers,[16] *e.g.*, A and B, the coupling constant J can be given by

$$J = (1/n_A n_B)\sum_{ij} J_{ij}$$

where J_{ij} is the contribution due to the interaction between the magnetic orbitals i on A and j on B, and n_I (I = A, B) is the number of unpaired electrons on the the centre I. In general, the pair contribution J_{ij} can be written as the sum of a ferromagnetic term $J_{ij}^F > 0$ and an antiferromagnetic term $J_{ij}^{AF} < 0$, *i.e.*, $J_{ij} = J_{ij}^F + J_{ij}^{AF}$. Using the model of localized orbitals developed by Kahn and co-workers,[16d] J_{ij}^F can be expressed in terms of the bielectronic exchange integrals $k_{ij} = \langle a_i(1)b_j(2)|1/r_{12}|a_i(2)b_j(1)\rangle$ as $J_{ij}^F = 2k_{ij}$, while J_{ij}^{AF} can be expressed in terms of the monoelectronic overlap integral $S_{ij} = \langle a_i(1)|b_j(1)\rangle$ as $J_{ij}^{AF} \propto S_{ij}^2$, i.e., the stronger the overlap the stronger the antiferromagnetic contribution. Orbitals orthogonal by symmetry will have zero overlap and will not give an antiferromagnetic contribution to J_{ij}. Usually the antiferromagnetic contributions are much larger than the ferromagnetic ones, so that often only one antiferromagnetic path (*i.e.*, a couple i, j for which $S_{ij} \neq 0$) is sufficient to overcome all the ferromagnetic contributions which lead to an overall antiferromagnetic coupling, $J < 0$. If, however, the orbitals are all orthogonal, then the overall interaction will be ferromagnetic, $J > 0$.

An analysis of the CN^- bridged Fe(III)−Mn(III) system (low spin d^5, t_{2g}^5; high spin d^4, t_{2g}^3, e_g^1) along these lines[17] would suggest the coexistence of both ferromagnetic and antiferromagnetic contributions and, since the antiferromagnetic contributions dominate, an overall antiferromagnetic coupling. Indeed, both ions have magnetic orbitals of t_{2g} symmetry which overlap and give rise to antiferromagnetic contributions. The unexpected ferromagnetic interactions observed in the metamagnetic compound **5** were explained in terms of the reduced overlap between the t_{2g} orbitals (d_{xz} and d_{yz}, taking the *z*-axis in the Fe−Mn direction) due to the rotation of the local *xy*-axis (defined as pointing toward the non-bridging ligands) around Fe and Mn by about 45°. However, the observed ferromagnetic interaction is the result of a subtle compromise between opposite ferromagnetic and antiferromagnetic contributions. Therefore, small changes in the geometry of the Fe−C−N−Mn unit could lead to significant changes and even to an inversion of the magnetic coupling between the two ions.

The main analogies and differences between the geometrical parameters of the two distinct Fe−CN−Mn units present in the $[Mn-NC-Fe-CN]_4$ tetramer of compounds **4** and **5** can be summarized as follows. (i) The Fe−C distances and Fe−C−N angles are similar for both units in the two compounds. (ii) In **4** both Mn−N distances (Mn−N(1), 2.266, Mn−N(2), 2.286 Å) and Mn−N−C angles (Mn−N(1)−C, 154.4°, Mn−N(2)−C, 146.6°) are similar; (iii) in **5** the two distinct Fe−CN−Mn units show relevant differences: the unit corresponding to the stronger intertrimer interaction has Mn−N = 2.290 Å and Mn−N−C = 169.5° while the unit corresponding to the weaker intertrimer interaction has Mn−N = 2.41 Å and Mn−N−C = 137.2°. Note that the Mn−N distance in **4** is similar to the intra-trimer Mn−N distance in **5** but the Mn−N−C angle is substantially more bent. On the other hand, the Mn−N−C angle in **4** is similar to the intertrimer Mn−N−C angle in **5** but the Mn−N distance is much shorter.

These two geometrical differences are expected to increase the overlap between the t_{2g} magnetic orbitals of the Fe(III) and Mn(III) species and may therefore explain the observed changes in the magnetic interactions: the bending of the Mn−C−N angle is important as it removes the strict orthogonality of the t_{2g} and e_g orbitals on different metals, thus introducing new antiferromagnetic paths, which overcome the ferromagnetic contribution.

Acknowledgment. This work was supported by the Ministry of Education, Science and Culture of Japan (N.M.), and the JSPS Research Fellowships for Young Scientists (H.M.). Foundation Herbette (University of Lausanne, N.R.) and Fonds National Suisse de la Recherche Scientifique (Bern, Switzerland, Grant 20-40268.94) are also acknowledged for financial support.

Supporting Information Available: Stacking of the adjacent two-dimensional layers of **4** along the *a*-axis, where the NEt_4^+ cation is positioned between the layers (Figure S1). Further details of the structure determination, including tables of atomic coordinates, anisotropic displacement parameters, bond lengths, bond angles, and nonbonded contacts (Tables S1−S5) for complex **4** (20 pages). Ordering information is given on any current masthead page.

IC9608814

(16) (a) Anderson, P. W. In *Magnetism*; Rado, G. T., Suhl, H., Eds.; Academic: New York, 1963; Vol. 1, p 25. (b) Goodenough, J. B. *Magnetism and the Chemical Bond*; Wiley: New York, 1963. (c) Hay, P. J.; Thiebault, J. C.; Hoffmann, R. *J. Am. Chem. Soc.* **1975**, *97*, 4884. (d) Kahn, O. In *Magneto-Structural Correlations In Exchanged Coupled Systems*; Gatteschi, D., Kahn, O., Willett, R. D., Eds.; Reidel: Dordrecht, The Netherlands, 1985; p 37.

(17) Mallah, T.; Thiebault, S. Verdaguer, M.; Veillet, P. *Science* **1993**, *262*, 1555.